Experimental Observation of Quasicrystal Growth

Keisuke Nagao,[1] Tomoaki Inuzuka,[1] Kazue Nishimoto,[2] and Keiichi Edagawa[1*]

[1]*Institute of Industrial Science, The University of Tokyo, Komaba, Meguro-ku, Tokyo 153-8505, Japan*
[2]*Institute of Multidisciplinary Research for Advanced Materials, Tohoku University, Sendai 980-8577, Japan*

The growth of an Al-Ni-Co decagonal quasicrystal was observed by *in situ*, high-temperature, high-resolution transmission electron microscopy. The tiling patterns extracted from a series of high-resolution transmission electron microscopy images were analyzed on the basis of the high-dimensional description of quasicrystalline structures. The analyses indicated that the growth proceeded with frequent error-and-repair processes. The final, grown structure showed nearly perfect quasicrystalline order. Our observations suggest that the repair process by phason relaxation, rather than local growth rule, plays an essential role in the construction of ideal quasicrystalline order in real materials.

Quasicrystals possess a long-range translational order named quasiperiodicity [1], in which the structure cannot be described simply by the repetition of a unit cell, as it could for conventional crystals. This fact raises the question of how quasicrystals can grow, in other words, how the atoms can arrange themselves to construct such a peculiar order. While crystals can grow simply by copying a unit cell via local atomic interactions, the growth of quasicrystals with quasiperiodic long-range order appears to require the atoms adhering to the growth front to obtain nonlocal structural information, which is physically implausible. This problem has attracted much attention ever since the first discovery of a quasicrystal in 1984 [2], and several theoretical growth models, which primarily apply to decagonal and icosahedral quasicrystals, have been proposed [3–10].

First, models have been created to illustrate the random aggregation of symmetric decagonal or icosahedral clusters, with the assumption that the clusters join together under some constraint to maintain orientational order [3–6]. Though these types of models show better translational correlations than one might expect, they are still not sufficient to explain the correlations observed experimentally. Elser *et al.* [6,7] have shown that the degree of order is greatly improved in their cluster-aggregating models by introducing an annealing region in the vicinity of the growth front.

Onoda *et al.* [8] have reported the discovery of an algorithm for growing a perfect 2D Penrose tiling by "local" rules, which is apparently inconsistent with Penrose's theorem [11], which states that Penrose tiling cannot be grown by local rules. This discrepancy can be resolved in view of different notions of locality in these rules [12]. Jeong [9] has extended Onoda's algorithm for the growth of a perfect 3D decagonal quasicrystal that consists of a periodic stacking of 2D Penrose tilings. Olami [10] has proposed a growth model for a pentagonal quasicrystalline tiling by local rules, generating highly

ordered quasicrystals with limited disorder in a tile arrangement, i.e., with limited phason disorder.

The problem of quasicrystal growth has been theoretically discussed in several studies, such as those mentioned above. In the present study, we performed *in situ*, high-temperature, high-resolution transmission electron microscopy (HRTEM) observations of the growth process of a quasicrystal.

An alloy with the composition $Al_{70.8}Ni_{19.7}Co_{9.5}$ was prepared from the elemental constituents by arc melting under an Ar atmosphere. The alloy was melt-spun using a single roller quenching apparatus. X-ray diffraction measurements showed that the melt-spun specimens consisted entirely of the decagonal quasicrystalline phase. The specimens were thinned by ion milling. Then, electron diffraction and transmission electron microscopy experiments, including *in situ* high-temperature HRTEM observations, were carried out using a 200-kV JEOL JEM-2010 F microscope equipped with a double-tilting heating stage. It was shown that the sample was polygrained with the basic Ni-type decagonal phase, which is known to have the best structural quality of all the decagonal quasicrystals [13]. Before heating, the grain size was typically 1.5 μm. The sample was heated to 1183 K at a heating rate of approximately 20 K/min, and it was held at this temperature. The grain growth process was observed by HRTEM at this temperature. The movie was recorded on a digital video disk at a rate of 30 frames/s. A series of images was extracted from the movie and analyzed. Details of the image-analysis procedure are given in the Supplemental Material [14].

Figure 1(a) shows an example of a HRTEM image taken at 1183 K, in which two grains, designated as *A* and *B*, are separated by a grain boundary indicated by the red curve. Electron diffraction experiments showed that both grains were of the decagonal phase but with different orientations. Any symmetry axes of grain *B* were far from the incident beam direction, resulting in a plain bright image with no
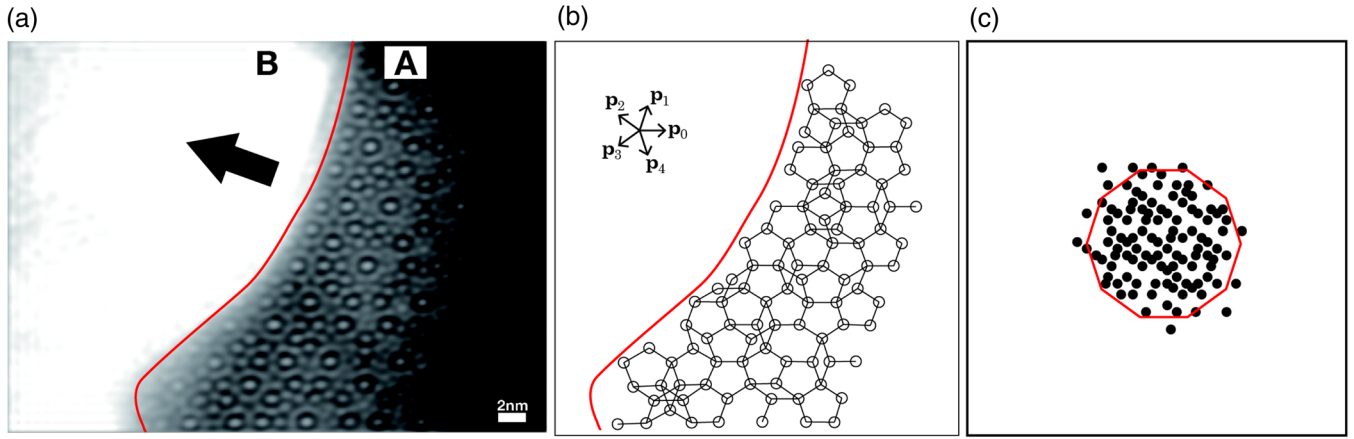
FIG. 1 (color online).   (a) An example of a HRTEM image taken at 1183 K, in which two grains, designated as A and B, are separated by the grain boundary indicated by the red curve. The growth direction of grain A is indicated by the arrow. For details of the image processing, see the Supplemental Material [14]. (b) The tiling pattern constructed by connecting the white spots in image (a) using the basis vectors $\mathbf{p}_i$ ($i = 0, ..., 4$). (c) The perp-space point distribution deduced from the tiling pattern in (b). The decagon indicates the domain for the pentagonal Penrose tiling.

contrast. On the other hand, the tenfold axis of grain A coincided with the incident beam direction, resulting in an arrangement of white spots on a black background. The experimental conditions for obtaining this sort of image have been described in our previous papers [15,16]. Here, each white spot is considered to represent the position of a columnar atomic cluster constituting the decagonal quasicrystalline structure.

In Fig. 1(b), a tiling pattern is constructed by connecting the white spots in the image of Fig. 1(a) using the basis vectors $\mathbf{p}_i = a(\cos(2\pi i/5), \sin(2\pi i/5))$ ($i = 0, ..., 4$) with $a \approx 2.0$ nm. This pattern resembles the pentagonal Penrose tiling that is one of the typical decagonal quasicrystalline tilings. Having selected a vertex in the tiling pattern as the origin, we can represent every vertex position $\mathbf{r}_\parallel$ as a linear combination of $\mathbf{p}_i$ ($i = 0, ..., 4$) with integer coefficients, i.e., $\mathbf{r}_\parallel = \sum_{i=0}^{4} n_i \mathbf{p}_i$. To ensure a one-to-one correspondence between $\mathbf{r}_\parallel$ and $(n_0, ..., n_4)$, we imposed the condition that $(n_0, ..., n_4)$ satisfy $\sum_{i=0}^{4} n_i = 0, \pm 1$, or ± 2. The procedure of determining a five-dimensional lattice point $(n_0, ..., n_4)$ from $\mathbf{r}_\parallel$ using the above relations is called "lifting." Projection of the lifted $(n_0, ..., n_4)$ onto the "perp space", which is defined as the space perpendicular to the real space, was performed by calculating $\mathbf{r}_\perp = \sum_{i=0}^{4} n_i \mathbf{q}_i$, where $\mathbf{q}_i$ are defined as $\mathbf{q}_i = \mathbf{p}_{(2i \bmod 5)}$. For ideal decagonal quasicrystalline tilings, the points $\{\mathbf{r}_\perp\}$ are distributed densely within a bounded domain. The points $\{\mathbf{r}_\perp\}$ deduced from the points $\{\mathbf{r}_\parallel\}$ in Fig. 1(b) are shown in Fig. 1(c). The decagon indicates the domain for the pentagonal Penrose tiling. The points $\{\mathbf{r}_\perp\}$ are mostly accommodated in the domain, indicating that the tiling pattern in Fig. 1(b) is close to an ideal quasicrystalline tiling.

We observed the process in which grain A in Fig. 1(a) grew in the direction indicated by an arrow in the figure by eating grain B. The movie of this process is presented in

the Supplemental Material [14]. Figures 2(a)–2(d) show the images at $t = 2.1, 4.9, 11.3,$ and 13.6 s, respectively, where the time was measured from the moment at which the image of Fig. 1(a) was taken. The results of the analyses of the image series extracted from the movie, including those in Figs. 2(a)–2(d), are presented below. Our main findings are as follows. During the growth process, the quasicrystalline order was not always maintained; the growth proceeded with frequent error-and-repair.

Figures 3(a)–3(c) present an example of such an error-and-repair process observed in this experiment. In the left column, the vertices of the tilings extracted from the images at $t = 4.9, 6.1,$ and 6.6 s are presented, and the lattice planes parallel to $\mathbf{p}_1$ are drawn. These lattice planes are perpendicular to the growth direction. The corresponding
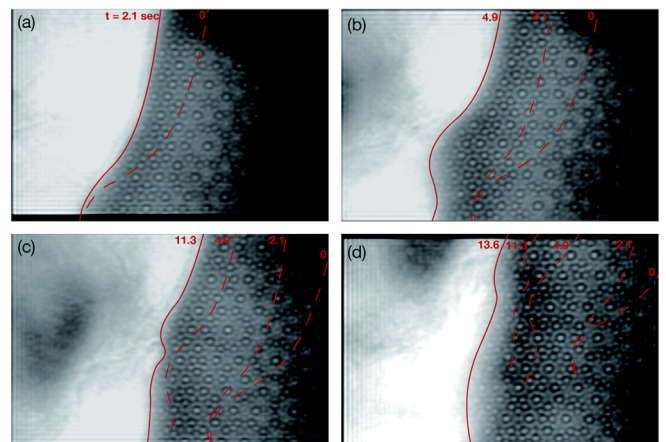

FIG. 2 (color online).   (a)–(d) The HRTEM images at $t = 2.1,$ 4.9, 11.3, and 13.6 s, respectively, where the time was measured from the moment at which the image in Fig. 1(a) was taken. The positions of the growth front at $t = 0, 2.1, 4.9, 11.3,$ and 13.6 s are indicated by red curves in the figures.
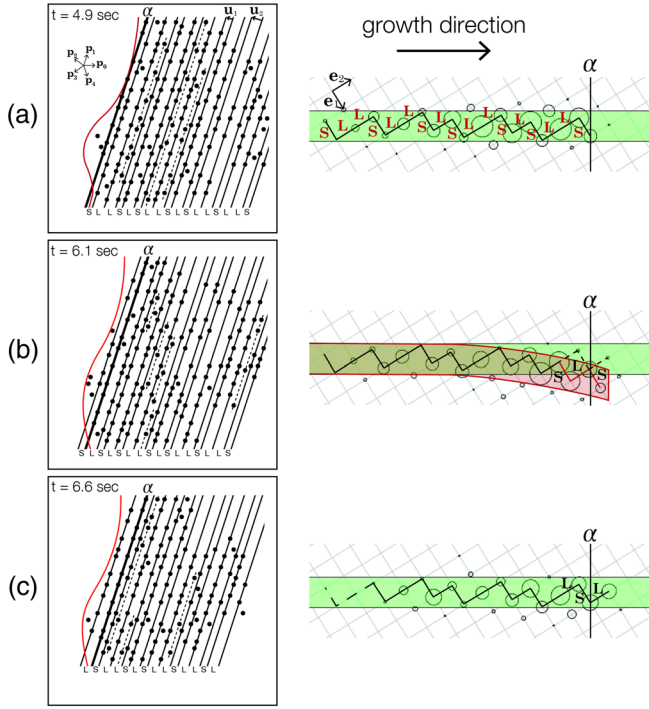
FIG. 3 (color online).   An example of an error-and-repair process. In the left column, the vertices of the tilings extracted from the images at $t = 4.9$ (a), 6.1 (b), and 6.6 s (c) are presented, and the lattice planes parallel to $\mathbf{p}_1$ are drawn. The lattice planes on which many vertices lie consist mostly of two different lattice spacings, L and S. In the right column, 2D maps of the lattice planes are shown (see text).

images are presented in the Supplemental Material [14]. In Fig. 3(a), the lattice planes on which many vertices lie consist mostly of two different lattice spacings: long (L) and short (S) ones, the ratio of which is the golden mean, $\tau = (1 + \sqrt{5})/2$. In the right column of Fig. 3(a), the arrangement of the lattice planes is analyzed. The position $\mathbf{t}$ of a lattice plane can be indexed by integers (m_1, m_2) as $\mathbf{t} = m_1\mathbf{u}_1 + m_2\mathbf{u}_2$, using the two vectors $\mathbf{u}_1 = (\mathbf{p}_3 - \mathbf{p}_4)/2$ and $\mathbf{u}_2 = (\mathbf{p}_2 - \mathbf{p}_0)/2$. Here, $\mathbf{u}_1$ and $\mathbf{u}_2$ are parallel to the growth direction, and $|\mathbf{u}_1| = S$ and $|\mathbf{u}_2| = L$, as shown in Fig. 3(a). The vertex of $(n_0, \ldots, n_4)$ lies on the lattice plane of $(m_1, m_2) = (n_3 - n_4, n_2 - n_0)$. In the right column of Fig. 3(a), the lattice planes (m_1, m_2) in the tiling structure are mapped to $\mathbf{T} = m_1\mathbf{e}_1 + m_2\mathbf{e}_2$ on a 2D lattice spanned by $\mathbf{e}_1$ and $\mathbf{e}_2$, where the size of the circle is proportional to the number of vertices on the lattice plane. The L-S sequence in the left column corresponds to the stairlike structure in the right column. If the tiling has a perfect decagonal quasicrystalline order, the L-S sequence should be a one-dimensional Fibonacci lattice. This behavior is demonstrated for the pentagonal Penrose tiling in the Supplemental Material [14]. The stairlike structure in Fig. 3(a) is accommodated within the green strip, which has a slope τ and width $|\mathbf{e}_1^\perp| + |\mathbf{e}_2^\perp|$, where the superscript $\perp$ denotes the projection of the vector onto a line

perpendicular to the strip direction. This fact indicates that the L-S sequence in Fig. 3(a) corresponds to a part of a Fibonacci lattice.

The stairlike structure in Fig. 3(a) indicates that L should be added to the last lattice plane (α) to keep the order. However, S has incorrectly been added at 6.1 s in Fig. 3(b). The new lattice plane is located well below the green strip in the 2D map. This incorrect attachment of the lattice plane induced additional tile rearrangement in the already-grown region. As a result, we could draw a bent strip to accommodate the 2D points of the lattice planes, as in the right-hand figure in Fig. 3(b). The bent strip indicates the introduction of phason strain. Subsequently, this phason strain had relaxed almost completely by $t = 6.6$ s, as shown in Fig. 3(c).

The degree of order in the lattice plane arrangement was evaluated by the deviation Δ of the weighted average of $\mathbf{T}^\perp$ (the projection of $\mathbf{T}$ onto the perp space) from the center of the green strip. The time dependence of the deviation is shown in Fig. 4(a). Within the 15 s observation, six error-and-repair events are evident, as shown with the shaded time regions. The error-and-repair event presented in Fig. 3 corresponds to the second one in Fig. 4(a). In the present
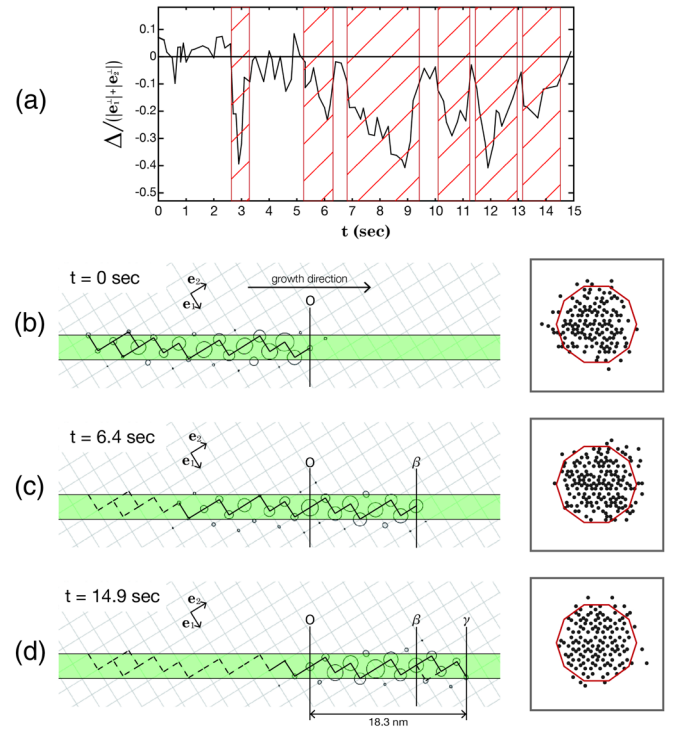

FIG. 4 (color online).   (a) Time dependence of the degree of order in the lattice plane arrangement, where $\Delta = 0$ corresponds to the ideal order. We find that Δ departs from and returns to zero, which corresponds to an error-and-repair event. Six such events are identifiable in the shaded time regions. (b)–(d) 2D maps of the lattice planes and perp-space point distributions at $t = 0$, 6.4, and 14.9 s, respectively, showing that the overall growth proceeds while maintaining a nearly perfect quasicrystalline order.

observation at 1183 K, the repair processes typically took 1 s, which should correspond to the phason-strain relaxation time. We observed the growth at various temperatures and found that the relaxation time was strongly temperature dependent. For example, at 1123 K, the typical relaxation time was 10–20 s, where the repair process was observed after several lattice planes had grown incorrectly.

It should be noted that all six events in Fig. 4(a) show the same direction of deviation: the peaks of Δ are all on the minus side. This result indicates that the error always occurred in such a way that S was added when L had been expected. This behavior may be due to the fact that, as the growth front proceeds from the last lattice plane, S becomes possible to be generated before L becomes possible.

Because the introduction of error is always followed by the repair process, the overall growth appeared to proceed while maintaining a nearly perfect quasicrystalline order. In Figs. 4(b)–4(d), 2D maps of the lattice plane arrangements extracted from the images at $t = 0$, 6.4, and 14.9 s are presented, together with the 2D distributions of $\{\mathbf{r}_\perp\}$. The corresponding images and vertices of the tilings are presented in the Supplemental Material [14]. We observed growth of approximately 18.3 nm during the 14.9 s time period. The stairlike structures of L and S are accommodated within a strip with slope τ and width $|\mathbf{e}_1^\perp| + |\mathbf{e}_2^\perp|$, indicating an ideal order.

In early years, all known quasicrystalline phases were metastable and could be obtained only by rapid quenching. These phases show considerable deviations from the ideal quasicrystalline order; they generally show diffraction peak widths that increase linearly with $|\mathbf{G}_\perp|$, the magnitude of the phason momentum. This behavior indicates that the root-mean-square phason fluctuations grow linearly with system size [17,18]. The models of the random aggregation of clusters generally show more rapid increases of peak width with $|\mathbf{G}_\perp|$ [5]. However, by introducing an annealing region in the vicinity of the growth front, some cluster aggregating models have been shown to exhibit a linear increase of peak width with $|\mathbf{G}_\perp|$ [6,7], in agreement with experiments.

Later, "ideal" quasicrystals with virtually no phason disorder were found to form in many alloy systems such as Al-Cu-Fe, Al-Cu-Ru, and Al-Pd-Mn for icosahedral quasicrystal, and Al-Ni-Co for decagonal quasicrystal. Some ideal growth models, such as those by Onoda et al. [8], Jeong [9], and Olami [10], can explain the formation of such ideal quasicrystals. These models incorporate no structural relaxation either during or after the growth; instead, the growth proceeds in a manner such that the quasicrystalline order is always maintained. This is qualitatively different from what we observed in the growth of the Al-Ni-Co decagonal quasicrystal. In our observations, incorrect tile attachments, i.e., introduction of phason defects occurred frequently during the growth, suggesting that no strict local growth rule is at work to force the construction of ideal quasicrystalline order. Frequent

introduction of errors (phason defects) during growth also indicates that the interactions among tiles, which should arise from atomic interactions, are local: nonlocal interactions would enable the growth of quasicrystal without errors. The phason defects, which are inevitably introduced during growth because of lack of nonlocal interactions, should increase phason elastic free energy, which can be relaxed through tile rearrangement by tile flips. This has actually been observed in our experiments. Thus, our observations demonstrate that this repair process by phason relaxation, rather than a local growth rule, plays an essential role in the construction of ideal quasicrystalline order in real materials. Here, local interactions appear to suffice to construct ideal quasicrystalline order through a phason relaxation process, as suggested by recent Monte Carlo [19] and molecular dynamics [20] simulations, in which quasicrystals are formed as thermodynamical equilibrium states only with local interactions.

It should be noted that even in the above-mentioned alloy systems, in which ideal quasicrystals form, rapid quenching leads only to the formation of disordered quasicrystals. Sufficient annealing after the solidification process is necessary to obtain ideal quasicrystals. Such ideal quasicrystals are also formed by sufficiently slow solidification processes, such as the Bridgman or Czochralski methods used to produce single-grain samples, in which phason relaxation should occur during the growth. The growth process observed in our experiment was even slower than in these methods, and therefore there was sufficient time for phason relaxation. In any case, repair by phason relaxation during or after growth should be involved to construct ideal quasicrystalline order in real materials.

In conclusion, we observed the growth process of an Al-Ni-Co decagonal quasicrystal by in situ high-temperature HRTEM. The tiling patterns extracted from a series of HRTEM images were analyzed on the basis of the high-dimensional description of quasicrystalline structures. The analyses indicated that the growth proceeded with frequent error-and-repair processes. The final, grown structure showed nearly perfect quasicrystalline order. Our observations suggest that repair by phason relaxation, rather than a local growth rule, plays an essential role in the construction of ideal quasicrystalline order in real materials. This is qualitatively different from the ideal growth models previously proposed.

*edagawa@iis.u-tokyo.ac.jp

[1] D. Levine and P. J. Steinhardt, Phys. Rev. B **34,** 596 (1986).

[2] D. Shechtman, I. Blech, D. Gratias, and J. W. Cahn, Phys. Rev. Lett. **53,** 1951 (1984).

[3] D. Shechtman and I. Blech, Metall. Trans. **16A**, 1005 (1985).

[4] P. W. Stephens and A. I. Goldman, Phys. Rev. Lett. **56**, 1168 (1986).

[5] P. W. Stephens, in *Apeiodicity, and Order 3*, edited by M. Jaric and D. Gratias (Academic Press, Boston, 1989) pp. 37–104.

[6] V. Elser, in *Apeiodicity, and Order 3*, edited by M. Jaric and D. Gratias (Academic Press, Boston, 1989) pp. 105–136.

[7] F. Nori, M. Ronchetti, and V. Elser, Phys. Rev. Lett. **61**, 2774 (1988).

[8] G. Y. Onoda, P. J. Steinhardt, D. P. DiVincenzo, and J. E. S. Socolar, Phys. Rev. Lett. **60**, 2653 (1988).

[9] H. C. Jeong, Phys. Rev. Lett. **98**, 135501 (2007).

[10] Z. Olami, Europhys. Lett. **16**, 361 (1991).

[11] R. Penrose, in *Introduction to Mathematics of Quasicrystals*, edited by M. V. Jaric (Academic Press, Boston, 1989). pp. 53–80.

[12] J. E. S. Socolar, in *Quasicrystals: The State of the Art*, edited by D. P. DiVincenzo and P. J. Steinhardt (World Scientific, Singapore, 1991) pp. 225–250.

[13] S. Ritsch, C. Beeli, H. U. Nissen, T. Godecke, M. Scheffer, and R. Luck, Philos. Mag. Lett. **78**, 67 (1998).

[14] See Supplemental Material at http://link.aps.org/supplemental/10.1103/PhysRevLett.115.075501 for details.

[15] K. Edagawa, K. Suzuki, and S. Takeuchi, Phys. Rev. Lett. **85**, 1674 (2000).

[16] K. Edagawa, K. Suzuki, and S. Takeuchi, J. Alloys Compd. **342**, 271 (2002).

[17] P. M. Horn, W. Malzfeldt, D. P. DiVincenzo, J. Toner, and R. Gambino, Phys. Rev. Lett. **57**, 1444 (1986).

[18] P. A. Heiney, P. A. Bancel, P. M. Horn, J. L. Jordan, S. LaPlaca, J. Angilello, and F. W. Gayle, Science **238**, 660 (1987).

[19] T. Dotera, T. Oshiro, and P. Ziherl, Nature (London) **506**, 208 (2014).

[20] M. Engel, P. F. Damasceno, C. L. Phillips, and S. C. Glotzer, Nat. Mater. **14**, 109 (2015).